Available online at www.sciencedirect.com

ScienceDirect

Journal of Photochemistry and Photobiology A: Chemistry 188 (2007) 155–160

Journal of Photochemistry and Photobiology A:Chemistry

www.elsevier.com/locate/jphotochem

Synthesis and characteristics of a novel rare earth complex of $Eu(TTA)_2(N\text{-}HPA)Phen$

Yuguang Lv[a,c], Jingchang Zhang[a,*,1], Weiliang Cao[a], Joon Ching Juan[a,d], Fujun Zhang[b], Zheng Xu[b]

[a] *Institute of Modern Catalysis, Beijing University of Chemical Technology, State Key Laboratory of Chemical Resource Engineering, Beijing 100029, China*
[b] *Institute of Optoelectronic Technology, Laboratory of Materials for Information Storage and Displays, Northern Jiaotong University, Beijing 100044, China*
[c] *Chemistry-Pharmacy College of Jiamusi University, Jiamusi 154007, China*
[d] *Advanced Catalysis Technology Laboratory, School of Chemical Sciences and Food Technology, Faculty of Science and Technology, Universiti Kebangsaan Malaysia, Bangi 43600, Malaysia*

Received 13 July 2006; received in revised form 25 November 2006; accepted 1 December 2006
Available online 3 December 2006

Abstract

Rare-earth four-fold compounds of Eu^{3+} with HTTA, N-HPA and 1,10-phenanthroline have been synthesized. The characteristic of the compounds have been studied by UV, IR, DTA–TG, XRD and fluorescence spectroscopy. The complex of Eu(III) emits strong red fluorescence when excited by UV light. UV absorption spectrum shows the absorption energy of complexes mostly from ligands. IR spectra suggest that complexes have been successfully synthesized. It is proved by TG curve that the complex is stable, ranging from ambient temperature to 210 °C in air. The organic–inorganic combined structural device (ITO/PVK: Eu/ZnS/Al) is fabricated based on layered optimization scheme. Europium (Eu) ions may also be excited by intramolecular energy transfer from ligands. There are two kinds of excitation mechanisms: impacted excitation and injected recombination for the combined structural device. The electroluminescence (EL) intensity of the combined structural device is strongly improved and reaches up to 381 cd/m^2 at 20 V compared with the pure organic structural device. It may be an effective method to improve the EL intensity of the lanthanide complex by using electric characteristics of inorganic semiconductor materials.

Keywords: $Eu(TTA)_2(N\text{-}HPA)Phen$; Synthesis; Photoluminescence; Organic electroluminescence

1. Introduction

Since the 1960s, $Eu(TTA)_3Phen$, $Sm(TTA)_3Phen$ complexes have attracted considerable attention because of their high luminescence emission efficiency, which owed to high absorption coefficient of HTTA and synergistic effect of 10-phenanthroline [1,2]. Rare earth (RE) metal complexes have some good characteristics, such as extremely narrow emission bands and high internal quantum efficiencies, which are suitable to use as the emission materials (in OEL) [3,4]. Therefore, many RE complexes have been synthesized and used as the emitters in organic photoluminescence and electroluminescence devices [5–8].

Throughout the last decade, the interest in electroluminescence of lanthanide (Ln) complexes was increased due to their attractive properties, such as long lifetime, large Stokes shift and line-like emission. However, since their f–f transition is inhibited due to spatial distribution of charge, they absorb very little excited energy [9–11]. So Ln(III) ions are chelated with ligands that have broad and intense absorption bands. The ligand absorbs energy or captures an electron–hole pair and then transfers it to the lanthanide ions. However, little attention has been paid to rare earth four-fold complexes with Eu^{3+}, HTTA, N-HPA and 1,10-phenanthroline.

In the paper, we report that there are two routes for the excitation of lanthanide ions based on the organic–inorganic combined structural device: (i) hot electrons directly impact

---

[*] Corresponding author. Tel.: +86 1 64434904; fax: +86 1 64434898.
E-mail address: zhangjc1@mail.buct.edu.cn (J. Zhang).

[1] Supported by the Research Fund for the Doctoral Pragram of Higher Education (No. 20050010014).

1010-6030/$ – see front matter © 2006 Elsevier B.V. All rights reserved.
doi:10.1016/j.jphotochem.2006.12.003

excitation the lanthanide ions through resonant energy transfer, (ii) ligand absorbs energy or captures an electron–hole pair and then transfers itself energy to the lanthanides ions through intramolecular energy transfer. It was found that there was an efficient energy transfer process between the ligands and metal ions when the device operating at low voltages. The combined structural device may be an effective way to improve the EL intensity of lanthanide ions.

2. Experimental

2.1. Materials

The purity of europium, terbium oxides was 99.99%, other reagents were analytical reagents.

2.2. Synthesis of materials RE(TTA)$_2$N-HPAPhen

One millimole of EuCL$_3$·6H$_2$O, 2 mmol of HTTA and 1 mmol of N-HPA were dissolved in 50 ml ethanol. The pH value of the mixture was adjusted to 6–7 by adding 3 mmol ammonia. Then, 1,10-phenanthroline in ethanol solution was added to the reaction mixture, the molar ratio of 1,10-phenanthroline to RE^{3+} ion being 1:1. The precipitation was filtered, washed with water and ethanol, dried at room temperature, and then stored in a silica-gel drier.

2.3. Measurements

DTA–TG curves were obtained on a TGA-DTA1700-Perkin-Elmer. Sample amount: 3.6 ± 0.2 mg; temperature scope: 25–900 °C; at a heating rate of 10 °C/min in air. X-ray diffraction (XRD) analysis was carried out using a D/MAX 2500 VB2+/PC. The conditions used were: Cu Kα radiation ($\lambda = 1.54056$ Å) at 40 kV and 200 mA, scanning angle (2θ) from 5° to 60° with step scan of 0.04° every second. The FTIR spectra of the samples were recorded on a Shimadzu FTIR-8400S by KBr pellet technique. The sample was ground with spectral grade KBr to form a mixture, which was then made into a pellet using a hydraulic press. This pellet was used to record the infrared spectra in the range 4000–400 cm^{-1}. UV–vis spectra were performed on a UV-2501PCS in the range of 400–200 nm. The EL spectra were measured by SPEX Fluorolog-3 spectrometer at room temperature. The luminance was measured by PR-650 spectra-scan spectrometer. The current–voltage characteristics of the devices were analyzed using a Keithley Source Meter 2410.

3. Results and discussion

3.1. DTA–TG analysis

DTA–TG spectrum of Eu(TTA)$_2$(N-HPA)Phen complex is shown in Fig. 1. For example, DTA spectrum of Eu(TTA)$_2$(N-HPA)Phen complex shows endothermic peak (melt-endothermic peak) at 215.5 °C but TG spectra of complex do not changed, and decomposition in two steps from 220 to 650 °C. TG curves prove that the complex is stable, ranging from ambient temperature to 210 °C in the air. Therefore, it is suitable to be used as the emission materials. From Table 1, it can be seen that the complexes contents (RE$_2$O$_3$%) are not significant different from the results of calculation according to the formula.

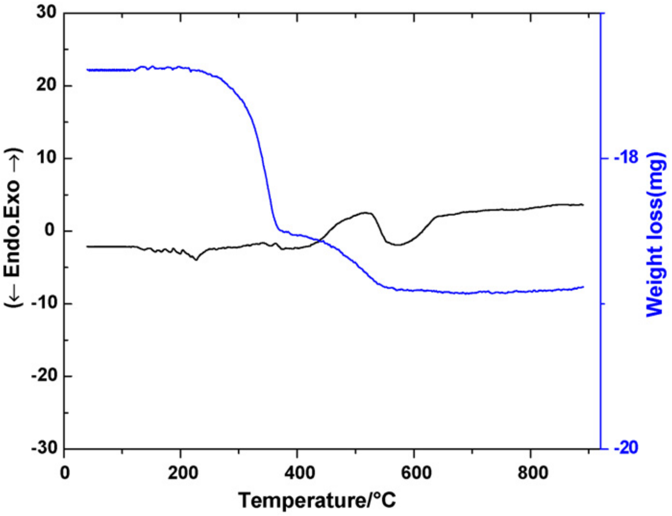

Fig. 1. DTA–TG spectra of four-fold complex of Eu(TTA)$_2$(N-HPA)Phen.

3.2. XRD analysis

XRD patterns of Eu(TTA)$_2$(N-HPA)Phen complex are shown in Fig. 2. Eu(TTA)$_2$(N-HPA)Phen complex has two high and incisive peaks (characteristic peaks) in $2\theta = 9$ and 22 °C.

3.3. IR spectra analysis

Special attention was paid to their IR around 2500–400 cm^{-1}. IR spectra of the typical Eu(TTA)$_2$(N-HPA)Phen complex is shown in Fig. 3. The peaks around 1539 cm^{-1} is corresponded to stretching vibration of –N=C (1,10-phenanthroline), 858 cm^{-1}, 721 cm^{-1} is corresponded to r$_{\text{C–H}}$ vibration of 1,10-

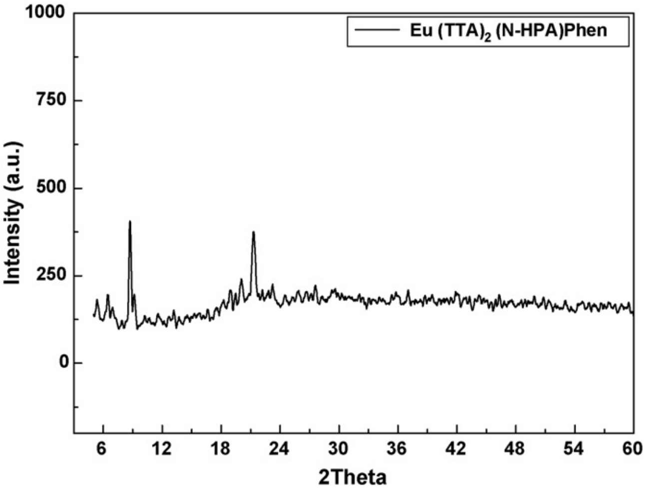

Fig. 2. XRD spectra of complex Eu(TTA)$_2$(N-HPA)Phen.

Table 1
DTA–TG peaks of complexes

	Decompose temperature/°C and weight loss (%)				RE_2O_3%
	T_{m1} (°C)	Weight loss (%)	T_{m2} (°C)	Weight loss (%)	Analytically found (calculated)
$Eu(TTA)_2$N-HPAPhen	215.5	0.00	521.1	75.7	16.9 (17.8)

phenanthroline and the peak in the spectra of complexes at about 540 cm^{-1} reveals the presence of C–O–RE and it cannot be observed in the ligands. In addition, typical asymmetric vibration of $V_{C=O}$ (TTA) group peaks were detected about 1603 and 1511 cm^{-1}, symmetric and asymmetric vibration of $-COO^-$(N-PA) group peaks was detected about 1577and 1413 cm^{-1}. IR spectrum of complex was obviously different from HTTA, N-HPA and 1,10-phenanthroline ligands. This indicates that were similar to the complex reported before [12,13]. It is concluded that $Eu(TTA)_2$(N-HPA)Phen complex has been synthesized, and the chemical structure is shown in Fig. 4.

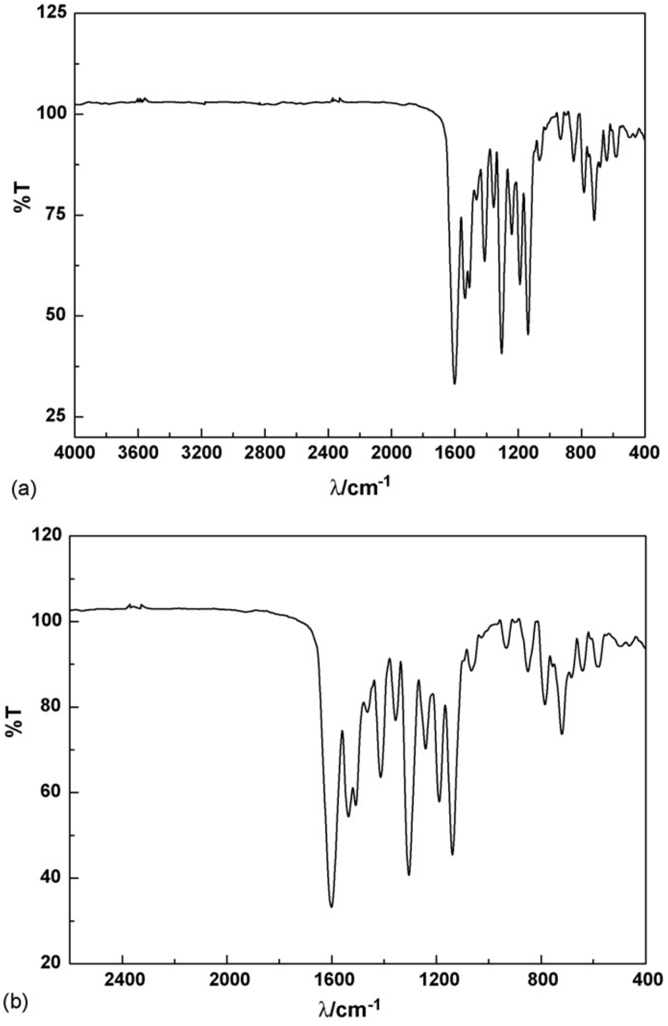

Fig. 3. (a) Infrared spectra of $Eu(TTA)_2$(N-HPA)Phen in the range 4000–400 cm^{-1}. (b) Infrared spectra of $Eu(TTA)_2$(N-HPA)Phen in the range 2500–400 cm^{-1}.

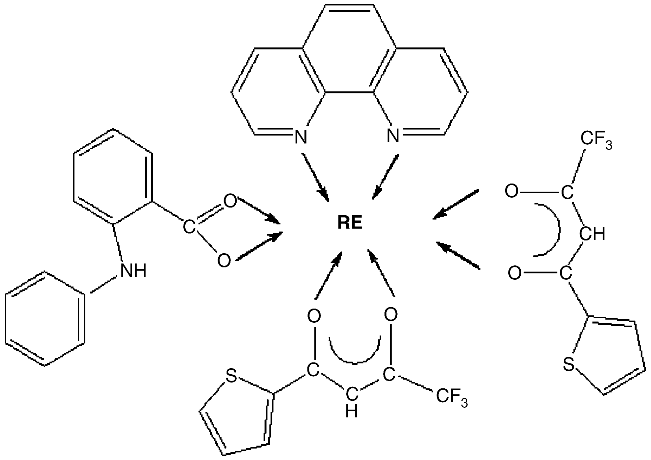

Fig. 4. Chemical structure of complex $Eu(TTA)_2$(N-HPA)Phen.

Table 2
Major UV absorption peaks of ligands and part complexes

HTTA	N-HPA	1,10-Phen	$Eu(TTA)_2$(N-HPA)Phen
λ_1 (354.80 nm)	λ_1 (384.80 nm)	λ_1 (324.50 nm)	λ_1 (339.30 nm)
λ_2 (344.80 nm)	λ_2 (357.20 nm)	λ_2 (291.20 nm)	λ_2 (271.50 nm)
λ_3 (324.00 nm)	λ_3 (295.40 nm)	λ_3 (268.00 nm)	

3.4. UV absorption spectra

UV absorption spectra peaks of free ligands and complex in $CHCl_3$ solution are listed in Table 2. Fig. 5 shows UV spectrum of complexes $Eu(TTA)_2$(N-HPA)Phen in different concentra-

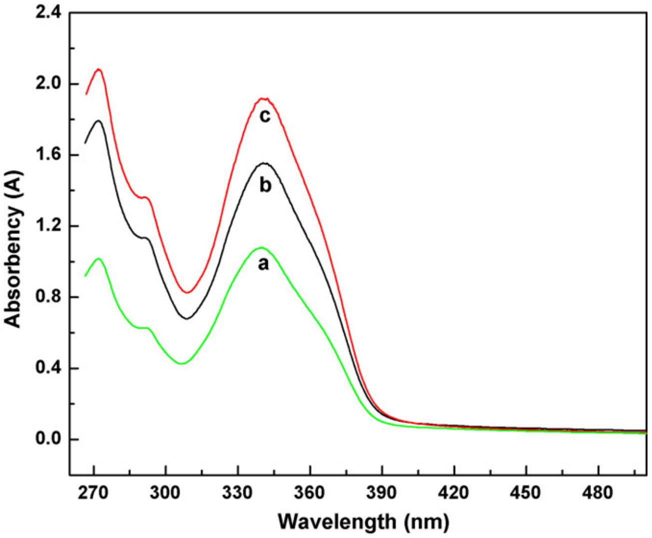

Fig. 5. UV spectra of complex $Eu(TTA)_2$(N-HPA)Phen.

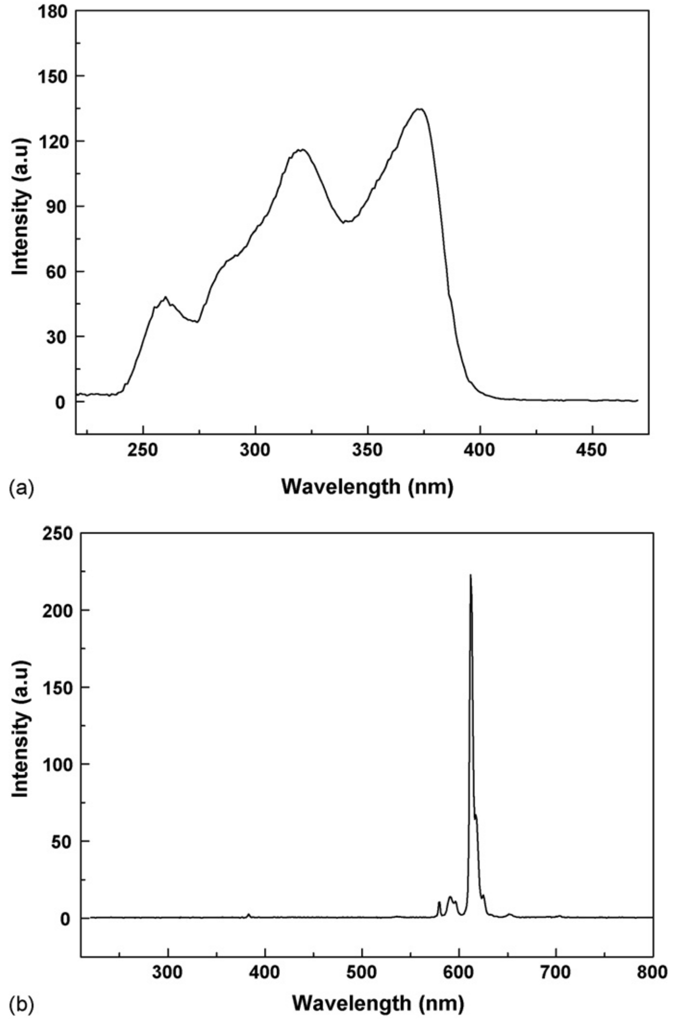

Fig. 6. (a) Typical excitation spectrum of complex Eu(TTA)$_2$(N-HPA)Phen. (b) Typical emission spectrum of complex Eu(TTA)$_2$(N-HPA)Phen.

tion (a 1×10^{-3} M, b 1×10^{-5} M and c 1×10^{-4} M), it can be seen that absorption peaks of Eu(TTA)$_2$(N-HPA)Phen complex is the strongest in 1×10^{-4} M. Absorption energy of the complex mostly comes from that ligands, Eu(TTA)$_2$(N-HPA)Phen shows typical absorptions peaks of HTTA, N-HPA and 1, 10-Phen.

3.5. Fluorescence properties

Excited spectra were recorded by monitoring Eu^{3+} luminescence at 613 nm. Emission spectra of complexes were obtained by exciting these complexes with ultraviolet (Fig. 6). Fluorescence excitation and emission spectra of Eu(TTA)$_2$(N-HPA)Phen complex is shown in Fig. 6. For the excitation spectrum consists of a symmetric and broad band, ranging from 240 to 400 nm ($\lambda_{max} = 385$ nm) with some small peaks superimposed with the band. The corresponding emission spectrum contains $^5D_0 \rightarrow {}^7F_j$ ($j = 0, 1, 2, 3, 4$) transition lines of Eu^{3+}, with hypersensitive transition $^5D_0 \rightarrow {}^7F_2$ red emission as the most prominent group.

3.6. Organic electroluminescence

The four-fold complex is Eu(TTA)$_2$(N-HPA)Phen, the ligands are N-HPA, HTTA and 1,10-Phen, which have been proven as an efficient luminescence of Eu^{3+} ion. Here, poly(*N*-vinylcarbazole) (PVK) was dissolved in chloroform with concentration 10 mg/ml. In order to improve the performance of Eu(TTA)$_2$(N-HPA)Phen thin film, Eu(TTA)$_2$(N-HPA)Phen was doped into PVK at weight ratio of 1:3. Indium tin oxide (ITO) coated glass substrates with a sheet resistance of 60 Ω/Sq. were cleaned consecutively in ultrasonic baths containing acetone, ethanol and DI-water. The PVK: Eu(TTA)$_2$(N-HPA)Phen thin film was fabricated on the top of cleaned ITO coated glass substrate by spin-coating method. 2,9-Dimethyl-4,7-dipheny l-1,10-phenanthroline (BCP) and aluminum quinoline (Alq$_3$) films were fabricated by thermal evaporation at a rate of about 0.3 Å/s under high vacuum of 2×10^{-6} Torr. ZnS thin film was prepared by electron beam evaporation at the growth rate of 0.5 Å/S under high vacuum of 2×10^{-6} Torr. The top Al electrode was prepared by thermal evaporation about 100 nm. The active emission area is about 2.25π mm^2. Two kinds of structural devices were fabricated and signed a symbol A and B, respectively.

Device A: ITO/PVK: Eu(TTA)$_2$(N-HPA)Phen (60 nm)/ZnS (80 nm)/Al.
Device B: ITO/PVK: Eu(TTA)$_2$(N-HPA)Phen (60 nm)/BCP (10 nm)/Alq$_3$(8 nm)/Al.

As we all know, BCP thin film is acted as a hole blocking layer and Alq$_3$ thin film is acted as an electron transporting layer for the device B. In the device A, semiconductor ZnS thin film is acted as electron function (transporting, acceleration) layer and hole blocking layer according to its electric characteristics and energy level instead of BCP and Alq$_3$ thin films in the device B. In the both structural devices, the characteristic emissions of europium ions at 594 nm, 615 nm, 655 nm and 690 nm are obtained under different driving voltage, as shown in Fig. 7. These emission peaks are corresponding to four energy level transitions of $^5D_0$–^7F_j ($j = 1, 2, 3, 4$) of europium ion (Eu^{3+}), respectively. The $^5D_0$–$^7F_1$ is magnetic dipole transition; $^5D_0$–^7F_j is an electric dipole transition whose intensity is sensitive to chemical environment. While the Eu ions are found at symmetrical center, $^5D_0$–$^7F_2$ has strong luminescence emission [14].

Fig. 7 shows EL spectra of device A and B under different driving voltage The EL intensity dependence on the driving voltage is obtained by using the time-base spectra. In the combined structural device, EL intensity abruptly increases when the driving voltage goes beyond 17 V, as shown in Fig. 8.

Why is the maximum EL intensity improved in the organic–inorganic combined devices compared with the pure organic structural device? We analyze the difference of the current density, the distribution of the internal electric field strength and the excitation mechanism for the two types of structural devices. In the combined structural device the electric field strength of the PVK layer is much larger than that of electron

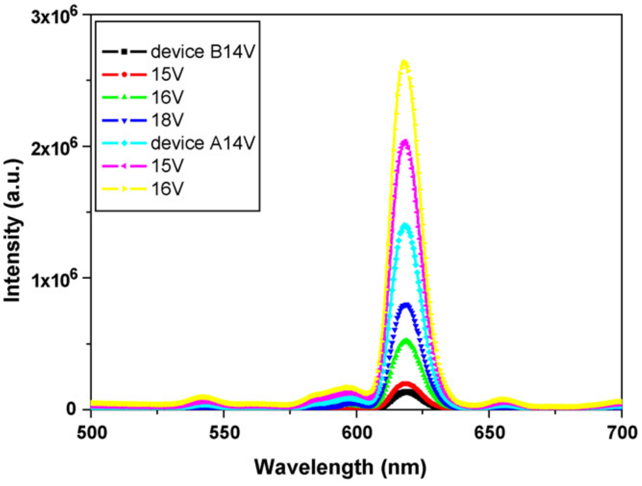

Fig. 7. EL spectra of device A and B under different driving voltage. (The comparison of relative EL intensity under different driving voltage is valid for the same device. But it is invalid for different devices because the measured conditions, such as relative position between device and photoelectric detector and the size of the slit, cannot be kept constant for different devices.)

function layer. It is the contrary for the pure organic structural device. The thickness of the PVK layer is the same for the two types of the structural devices. So the electric field strength of the PVK layer in the combined structural device must be larger than that in pure organic structural device under the same driving voltage. The bigger is the number of injected holes and electrons, the bigger is the probability to form exciton. For the combined structural device, the hole current density is increased because the majority of driving voltage drops across the PVK layer. It may be one reason for the improvement of EL intensity of the combined device.

Why is the current of the combined structural device much larger than that of the pure organic structural device, as shown in Fig. 9 We study the electron current and hole current for two types of structural devices. The electron current in the combined device is much larger than in the pure organic structural device due to the drastically different electron mobility. Another important reason is the influence of the electric field strength in the PVK layer on hole current. The electric field strength of the PVK layer in the combined structural device is larger than that in the pure organic structural device under the same driving voltage. So the hole current in the combined structural device is larger than that in the pure organic structural device.

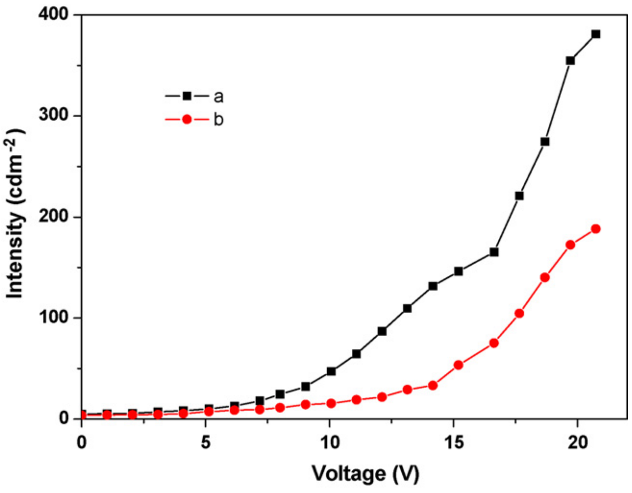

Fig. 8. EL luminance dependence on the driving voltage.

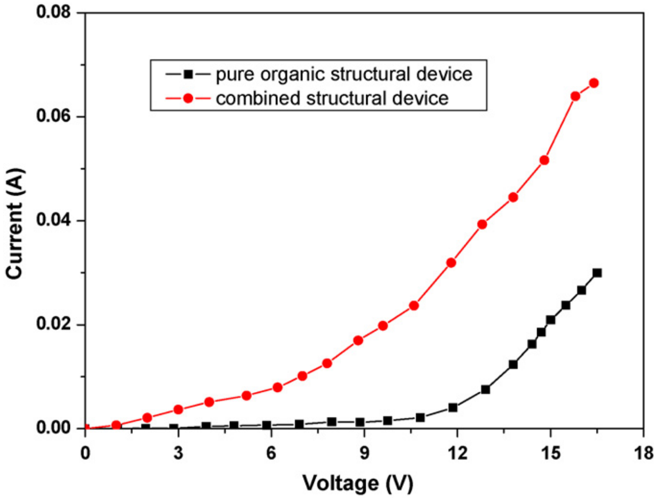

Fig. 9. Current–voltage curves for the two types of structure devices.

Obviously all these three kinds of electrons might recombine with injected holes from the anode. So in the combined structural devices, the excitation mechanism may include impacted excitation and injected recombination. Hot electrons play an important role in terms of EL intensity of lanthanide complex improvement [15,16].

4. Conclusions

Following conclusions can be drawn from this works:

(1) Rare-earth four-fold compound of Eu^{3+} with HTTA, N-HPA and 1,10-phenanthroline had been synthesized and used as emission materials. The experiment result shows the complex is stable, and their PL and EL properties were systematically studied by using these complexes as emissive materials.

(2) In the combined structural device, the semiconductor material ZnS thin film is used as an electron function (transporting and acceleration) layer instead of BCP and Alq_3 layers in the pure organic structural device. The majority of the driving voltage drops across the PVK layer because charge carrier mobility of ZnS is much larger than that of PVK. So the hole current density must be increased due to the increase of the electric field strength in PVK layer. These energetic electrons which have been accelerated in ZnS layer maintain their number invariant even though they lose their energy during the excitation of lanthanide complex or PVK. There are two kinds of excitation mechanisms: impacted excitation and injected recombination in the combined structural device. For the combined structural device, the EL luminance is strongly improved and reached up to

381 cd/m^2 at 20 V compared with the pure organic structural device. It can be used to design a new organic EL materials and a new type EL device configuration.

Acknowledgments

This work was supported by Institute of Optoelectronic Technology Beijing Jiao Tong University and Research Fund for the Doctoral Pragram of Higher Education (No. 20050010014).

References

[1] J.C.G. Bünzli, G. Bernardinelli, G. Hopfgartner, A.F. Williams, J. Am. Chem. Soc. 115 (1993) 817.
[2] J. Kide, H. Hayase, K. Hongawa, et al., J. Appl. Phys. Lett. 65 (1994) 2124.
[3] G. Sun, W. Li, Y. Zhao, et al., J. Lumin. 17 (1996) 364.
[4] Z.J. Wang, B. Li, Y. Fan, et al., J. Lumin. 17 (1996) 276.
[5] F. Di, C. Bei, W. Li, et al., J. Rare Earths 22 (2004) 334.
[6] G.-L. Zhong, J. Thin Solid Films 385 (2001) 234.
[7] G.-L. Zhong, J. Lumin. 99 (2002) 213.
[8] A.B. Li, Y. Yansheng, et al., J. Rare Earths 21 (2003) 514.
[9] D. Parker, Chem. Soc. Rev. 33 (2004) 156.
[10] N. Sabbatini, M. Guardigli, J.-M. Lehn, Chem. Rev. 123 (1993) 201.
[11] J.-C.G. Bünzli, C. Piguet, Chem. Rev. 102 (2002) 1897.
[12] X.-Q. Liang, N. Zeng, J. Guangxi University 26 (2001) 298.
[13] Y. Liua, C. Yeb, G. Qiana, J. Qiua, M. Wang, J. Lumin. 118 (2006) 158.
[14] S. Hong, Z. Xu, et al., J. Rare Earths 21 (2003) 519.
[15] F. Zhang, Z. Xu, F. Teng, L. Liu, L. Meng, Er Phosphor Mater. Sci. Eng. B 123 (1) (2005) 84–86.
[16] F. Zhang, Z. Xu, F. Teng, J. Lumin. 117 (2006) 90–94.